| OF |
AD
A054237

MICROCOPY RESOLUTION TEST CHART

NATIONAL BUREAU OF STANDARDS-1963-A

AFFDL-TR-77-113

FOR FURTHER TRAN~~~~

AD A054237

INVESTIGATION OF TEST FACILITY EFFECTS ON THE THREE-DIMENSIONAL BOUNDARY LAYER INTERACTION

Aeromechanics Division
High Speed Aeroperformance Branch

November 1977
TECHNICAL REPORT AFFDL-TR-77-113
Final Report for Period January 1977 to April 1977

D D C
RECEIVED
MAY 25 1978
E

Approved for public release; distribution unlimited

AIR FORCE FLIGHT DYNAMICS LABORATORY
AIR FORCE WRIGHT AERONAUTICAL LABORATORIES
AIR FORCE SYSTEMS COMMAND
WRIGHT-PATTERSON AIR FORCE BASE, OHIO 45433

NOTICE

When Government drawings, specifications, or other data are used for any purpose other than in connection with a definitely related Government procurement operation, the United States Government thereby incurs no responsibility nor any obligation whatsoever; and the fact that the government may have formulated, furnished, or in any way supplied the said drawings, specifications, or other data, is not to be regarded by implication or otherwise as in any manner licensing the holder or any other person or corporation, or conveying any rights or permission to manufacture, use, or sell any patented invention that may in any way be related thereto.

This report has been reviewed by the Information Office (OI) and is releasable to the National Technical Information Service (NTIS). At NTIS, it will be available to the general public, including foreign nations.

This technical report has been reviewed and is approved for publication.

Jerold L. Patterson

JEROLD L. PATTERSON
Project Engineer

FOR THE COMMANDER

Alfred C. Draper

ALFRED C. DRAPER
Asst. for Research and Technology
Aeromechanics Division

"If your address has changed, if you wish to be removed from our mailing list, or if the addressee is no longer employed by your organization please notify AFFDL/STINFO ,W-PAFB, OH 45433 to help us maintain a current mailing list".

Copies of this report should not be returned unless return is required by security considerations, contractual obligations, or notice on a specific document.

AIR FORCE/56780/23 March 1978 — 100

REPORT DOCUMENTATION PAGE		**READ INSTRUCTIONS** **BEFORE COMPLETING FORM**
1. REPORT NUMBER AFFDL-TR-77-113	2. GOVT ACCESSION NO.	3. RECIPIENT'S CATALOG NUMBER
4. TITLE *(and Subtitle)* INVESTIGATION OF TEST FACILITY EFFECTS ON THE THREE-DIMENSIONAL BOUNDARY LAYER INTERACTION.		5. TYPE OF REPORT & PERIOD COVERED Final Report. Jan 1976 to Apr 1977.
		6. PERFORMING ORG. REPORT NUMBER
7. AUTHOR(s) Jerold L. Patterson		8. CONTRACT OR GRANT NUMBER(s)
9. PERFORMING ORGANIZATION NAME AND ADDRESS Air Force Flight Dynamics Laboratory High Speed Aero Performance Branch (FXG) Wright-Patterson Air Force Base, Ohio 45433		10. PROGRAM ELEMENT, PROJECT, TASK AREA & WORK UNIT NUMBERS Project No. 1366 Task No. 136603 Work Unit No. 13660334
11. CONTROLLING OFFICE NAME AND ADDRESS Air Force Flight Dynamics Laboratory Aeromechanics Division (FX) Wright-Patterson Air Force Base, Ohio 45433		12. REPORT DATE November 1977
		13. NUMBER OF PAGES 63
14. MONITORING AGENCY NAME & ADDRESS*(if different from Controlling Office)*		15. SECURITY CLASS. *(of this report)* Unclassified
		15a. DECLASSIFICATION/DOWNGRADING SCHEDULE

16. DISTRIBUTION STATEMENT *(of this Report)*

Approved for public release; distribution unlimited.

17. DISTRIBUTION STATEMENT *(of the abstract entered in Block 20, if different from Report)*

18. SUPPLEMENTARY NOTES

19. KEY WORDS *(Continue on reverse side if necessary and identify by block number)*

Three-dimensional Interaction
Turbulent Boundary Layer
Wind Tunnel Test Data
Test Facility Effects

20. ABSTRACT *(Continue on reverse side if necessary and identify by block number)*

A continuing uncertainty when correlating three-dimensional shockwave/turbulent boundary layer interaction data obtained from different wind tunnel facilities is the extent of "facility-peculiar" effects on the test data, particularly the effect of free-stream Reynolds number. The present study investigates the pressure and heat transfer data in the interaction region taken at Mach 3 in three different facilities to determine the degree of dependency of the data on facility effects.

over

DD FORM 1473 EDITION OF 1 NOV 65 IS OBSOLETE
1 JAN 73

The study shows that, for constant Mach number, the interaction data are essentially independent of facility effects or can be made independent through proper modification.

The report also provides general data illustrating the physics of the interaction process for comparison with previous studies and to add to the general data base on three-dimensional interactions.

FOREWORD

This document presents the results of an experimental and analytical investigation of the effect of wind tunnel test facility on the characteristics of the three-dimensional shock wave/turbulent boundary layer interaction. The study was conducted by the High Speed Aero Performance Branch (FXG), Aeromechanics Division, Air Force Flight Dynamics Laboratory, Wright-Patterson Air Force Base, Ohio. The work was performed under Project 1366, "Aeroperformance and Aeroheating Technology;" Task 136603, Aerodynamic Heating to Military Vehicles;" Work Unit 13660334, "Interference Heating to Modular Missile Configurations." This report covers work conducted from January 1977 to May 1977.

ACCESSION for		
NTIS	White Section	☒
DDC	Buff Section	☐
UNANNOUNCED		☐
JUSTIFICATION		
BY		
DISTRIBUTION/AVAILABILITY CODES		
Dist.	AVAIL. and/or SPECIAL	
A		

AFFDL-TR-77-113

TABLE OF CONTENTS

LIST OF ILLUSTRATIONS

LIST OF ILLUSTRATIONS (CONTINUED)

LIST OF ILLUSTRATIONS (CONCLUDED)

LIST OF SYMBOLS

M	Mach number
$M_{N_{SH}}$	$M_\infty \sin \Theta$ (Figures 36 & 37)
P	Static pressure (psia)
Re	Reynolds number
St	Stanton number
X,Y	Coordinates as shown in Figure 6 (in.)
α	Fin deflection angle (radians)
δ	Boundary layer thickness (in.)
Θ	Shock angle (deg.)
ϕ	Angular location as shown in Figure 22 (deg.)
ψ	Fin deflection angle (deg.)

Subscripts

FP,F.P., u	Undisturbed, flat plate values
inc.	Incipient separation
∞	Free stream values
LE, L.E.	Leading edge values
onset	Onset of separating disturbance
PK	Peak value
PL	Plateau value
sep	Separated flow
SH	Shock wave value

SECTION I

INTRODUCTION

The three-dimensional interacting flow field caused by the impingement of an oblique shock wave on a turbulent boundary layer has been investigated extensively during the past several years. The interest in this interacting flow field stems from the now well known fact that the aerodynamic heating rates and pressures in the interaction region are several times greater than for an undisturbed flow. The shock wave/boundary layer interaction can be idealized through the flow model shown in Figure 1. The model consists of a sharp leading edge vertical fin mounted on a sharp leading edge flat plate in such a position that the oblique shock wave generated by the vertical fin impinges on the flat plate. Judicious placement of pressure and heat transfer instrumentation on the flat plate allows the surface effects of the interaction to be investigated. Figure 2 illustrates the typical characteristics of the interaction and shows typical pressure and heat transfer profiles in a plane normal to the undisturbed flow direction. Practical applications of this type of interacting flow field are associated with the junctures of wings, control surfaces, and engines with the aircraft fuselage. Detailed knowledge of the interacting flow field is necessary to allow development of methods to predict the heating rates and pressures on actual aircraft at flight conditions.

Intensive study of the three-dimensional shock wave/turbulent boundary layer interaction began approximately 10 years ago with the work of Stanbrook, McCabe, and Lowrie (References 1, 2, and 3). Neumann and Burke (Reference 4) were among the first to successfully develop a

1

technique to predict peak heating in a 3-D interaction, relating peak heating to peak pressure on the surface. Hayes (Reference 5) has recently extended and improved the prediction of both peak pressure and peak heating through his compilation and analysis of test results from several different facilities at Mach numbers ranging from three to six. Other investigations of prediction methods have been carried out by Neumann and Token (Reference 6), Korkegi (References 7 and 8), Holden (Reference 9), and more recently, by Scuderi (Reference 10) and Hayes (Reference 5) who have both developed methods for predicting pressure and heat transfer distributions across the interaction region as well as peak values.

The investigations of the three-dimensional interaction have been carried out in several different facilities including the AEDC Von Karman tunnels "A" & "B", the Langley UPWT, the AFFDL Mach 6, and the Princeton high Reynolds number facilities. A continuing uncertainty when comparing and correlating data from the various facilities is the extent of "facility-peculiar" effects on the test data, particularly the effect of flow Reynolds number. The primary purpose of the present study is to analyze the pressure and heat transfer data from three different test facilities at the same Mach number to determine the degree of dependency of the data on flow Reynolds number as a function of the particular facility being used. The data used for this purpose were at Mach 3. The goal was to show either that the data are essentially independent of facility effects as long as the Mach number is the same or, that the data can be modified in such a way that facility effects are cancelled out. The secondary purpose of this study was to provide data illustrating

the physics of the interaction process for comparison with previous Mach 3.7 results (Reference 6) and to add to the general body of information on three-dimensional interactions. The purpose of this report is to present the results of the above described investigation. The three test programs from which the Mach 3 data were obtained will first be described, followed by a discussion of the results of the data analysis and the conclusions drawn from the study.

SECTION II

DESCRIPTION OF TEST PROGRAMS

The wind tunnel data used in this investigation were obtained from test programs run at Arnold Engineering Development Center (AEDC), the NASA Langley Research Center, and Princeton University. The wind tunnel models used and the test conditions for each test program will be described in this section.

1. NASA LANGLEY RESEARCH CENTER TEST PROGRAM

The Langley Research Center test program utilized a large flat plate model 72 inches long and 52 inches wide mounted vertically on 20 inch high standoffs on the Unitary Plan Wind Tunnel sidewall. The model spanned the entire height of the wind tunnel. A remotely operated fin 24 inches long and 9 inches high was mounted on the plate. This model is shown in Figure 3. The model was tested at free-stream Mach numbers of 3.0 and 3.7, and unit Reynolds numbers of 1.50×10^6 per foot and 3.5×10^6 per foot. Surface static pressures and heat transfer data were obtained for fin incidence angles of up to 20°.

2. AEDC TEST PROGRAM

The AEDC test program employed a flat plate model 18 inches long and 10 inches wide. A fin 7.5 inches long and 3 inches high was mounted on the plate. This model is shown in Figure 4. The model was tested in AEDC-VKF tunnel "A" at a free-stream Mach number of 3.0 and unit Reynolds number of 3.25×10^6 per foot. Surface static pressure and heat transfer data were obtained for fin incidence angles

4

of up to 10°. This model was also tested at Mach 3.75 and 4.5 in Tunnel "A" and at Mach 4.75 and 5.04 in AEDC-VKF Tunnel "B". These additional test programs are discussed in References 5 and 6.

3. PRINCETON UNIVERSITY TEST PROGRAM

The Princeton University test program utilized a sharp flat plate, 8 inches wide by 10 inches long, mounted vertically between the top and bottom walls of the high Reynolds number boundary layer channel. The angle of incidence of the flat plate could be remotely adjusted. The Princeton model configuration is shown in Figure 5. The model was tested at a Mach number of 2.9 and a unit Reynolds number of 1.92×10^7 per foot. Surface static pressures and heat transfer were obtained for plate deflection angles of up to 14°.

SECTION III

DISCUSSION OF RESULTS

1. FACILITY DEPENDENCY OF INTERACTION DATA

The facility dependency of the three-dimensional interaction data will be discussed based on the surface measurements of static pressure and heat transfer.

The distributions of surface pressure and heat transfer across the interaction region and normal to the undisturbed flow direction have been plotted in the coordinate system shown in Figure 6. This coordinate system was shown in Reference 6 to be the best method for comparing data from diverse model configurations and facilities on a comparable non-dimensional basis.

It is not the intent of this report to discuss the shapes of the pressure and heat transfer profiles. The features of these profiles have been discussed in depth in References 5, 6, and 10.

a. Surface Static Pressure Distribution

Surface static pressure distribution for the three sets of test data were compared at as nearly equal physical distances downstream from the fin or shock generator leading edge as possible to cancel out pressure differences due to flow length effects. The pressures were then nondimensionalized using the static pressure measured in the undisturbed flow outside of the interaction region. The data location was also nondimensionalized by dividing the y-distance of the pressure tap location by the x-distance from the

leading edge. This was found to be a successful way to eliminate model scale effects. Figures 7 through 10 show a comparison of Langley and Princeton pressure data at a distance of approximately 7.5 inches from the fin leading edge for fin deflection angles of 4, 8, 10, and 12 degrees. It can be seen from these figures that the data correlation is excellent. Figures 11 through 13 show a similar comparison for the Langley and AEDC pressure data. These data sets do not correlate quite as well because the instrumentation was not located at as nearly equal distance from the fin leading edge as for the Langley and Princeton data. Thus, some Reynolds number effects are still apparent. Overall, however, the three sets of data agree well enough to conclude that the pressure distributions are essentially independent of facility effects and flow Reynolds number if flow length is constant. The Langley data were used as the standard against which the Princeton and AEDC data were plotted only because there were no instrumentation locations for which the Princeton and AEDC data could be compared directly. This was not meant to imply that the Langley data was any better, or worse, than the other two sets. The solid line through the Langley data is not a theory line but is intended only to help differentiate between the data sets.

Figures 7 through 13 also show the peak pressures predicted by the methods of Hayes (Reference 5) and Scuderi (Reference 10). The theory of Hayes provides slightly better predictions of peak pressures, particularly with increasing fin deflection angle.

b.   Surface Heat Transfer Data

Hayes in Reference 5 has shown that heat transfer data from diverse model configurations and facilities can be correlated most successfully by comparing data from comparable "X/δ" locations. The parameter "X/δ" is the ratio of the distance downstream of the fin leading edge to a reference boundary layer thickness. This is the method used for comparing the three sets of heat transfer data considered in this study. The reference boundary layer thickness for the AEDC and Princeton data was taken as the boundary layer thickness at the fin leading edge since the thickness was nearly constant over the instrumented portion of the flat plate. The reference thickness for the Langley data was taken to be the local boundary layer thickness for the particular gage row being considered because experimental measurement showed significant variation in thickness over the instrumented area of the flat plate. The heat transfer data were nondimensionalized using the heating rate measured in the undisturbed flow region outside of the interaction region and the data location was nondimensionalized in the same manner as for the pressure data. Figures 14 through 17 show a comparison of Langley and Princeton heat transfer data for an $X/\delta \cong 10$ and fin deflection angles of 4, 8, 10, and 14 degrees. The data plots show that in spite of an instability in the Princeton data, the data trends correlate quite well. Figures 18 through 20 show the similar comparison for the Langley and AEDC data for an $X/\delta \cong 20$ and fin deflection angles of 4, 8, and 10°. The plots show the AEDC data to be much smoother

8

than the Princeton data and the correlation with the Langley data
to be reasonably good. It will be noted that the AEDC data for a
fin deflection of 4 degrees apparently does not reach a peak (Figure
18). This is due only to gage placement on that row (Row 3). Peak
data were reached on later rows. The previous comments on the use
of the Langley data as the standard for comparison and on the solid
line through the Langley data apply for the heat transfer data in
the same manner as for the pressure data.

Figures 14 through 20 also show the peak heat transfer pre-
dicted by the methods of Hayes (Reference 5) and Scuderi (Reference 10).
The method of Scuderi seems to have a slight edge in accuracy par-
ticularly at the higher fin deflection angles. To further compare
the accuracy of these two prediction methods, Langley peak heating
data for $X/\delta \cong 10$ and $X/\delta \cong 38$ for fin deflection angle up to $20°$
were plotted. In this case, nondimensionalized heat transfer data
were plotted as a function of "$M_\infty \sin \Theta$" where Θ is the shock angle.
The parameter "$M_\infty \sin \Theta$" is the component of the free stream Mach
number normal to the oblique fin shock and is a measure of shock
strength. This parameter is another of those parameters found by
Hayes in Reference 5 to provide the most successful correlation of data
from different models and facilities. These heat transfer data are
shown in Figure 21. The plot shows that Hayes method provides much
better correlation with wind tunnel data, particularly for values
of $M_\infty \sin \Theta$ less than 1.5 (or equivalently, fin deflection angles
less than approximately 12 degrees).

9

2.   PHYSICAL CHARACTERISTICS OF THE MACH 3 INTERACTION

As stated earlier, the secondary purpose of this investigation
was to provide data illustrating the physics of the three-dimensional
interaction process at Mach 3 to add to the general body of infor-
mation on shockwave - turbulent boundary layer interactions. The
data to be presented here have been divided into two groups. The
first group illustrates the physical, or geometric, characteristics
of the interaction region (i.e., shock shapes, separation location,
peak heating location, etc.). The second group of data illustrates
the surface effects of the interaction process (i.e., surface pressures
and heating rates). The data will be presented with minimal inter-
pretation and analysis, or comparison to data from other sources.

a.   Geometric Data

The geometric characteristics of the interaction region
are shown in Figures 22 through 33. Figure 22 shows the angular
location of disturbance onset, separation, and the shock wave (see
Figure 2) for all three sets of data for a fin deflection angle of
10 degrees. Figure 23 shows the relative locations of peak pressure
and peak heating. As explained in References 5 and 6, and illustrated
in Figure 2, the inner heating peak should occur at approximately
the same location as the pressure peak. Each symbol in Figure 23
represents the normalized peak pressure (Y/X) location versus the
normalized peak heating location for a particular X/δ distance down-
stream from the fin leading edge and, while the values of Y/X will

10

change depending on X/δ, the ratios of Y/X should be approximately
1.0 if the locations of the inner heating peak and pressure peak do
coincide. Figure 23 shows that this is, indeed, the case. The
Langley data are not included because surface pressure measurements
were not taken at the same location as heat transfer (the model has
alternating rows of pressure taps and thermocouples spaced three
inches apart). Figure 24 shows the angular location of separation
(again see Figure 2) as a function of fin deflection angle for a
value of $X/\delta = 20$. The fin and fin shock locations are also shown
for reference. The Princeton data were not included in this plot
because the separation point was determined from the heat transfer
data and the Princeton data were too unstable to determine the
location of the outer heating peak associated with separation. Note
that Korkegi's incipient separation correlation ($M_\infty \alpha_{inc.} = 0.3$
from Reference 7) is also shown in this figure. Figure 25 shows a very
limited amount of data comparing the location of the separation point
with the point of onset of the inner heating peak. Neumann and Token
in Reference 6 found that the Y-location of these two points coincided in
the 3-D interaction. In the present investigation this was true also
of the AEDC data. However, for the Langley and Princeton data, the
value of St/St_u for the trough between the two peak heating points
was generally less than 1.0 so that the location of the point of on-
set of the inner heating peak could not be located by extending the
heating curve to the $St/St_u = 1.0$ line as shown in Figure 25. Fig-
ures 26 through 28 give the shock location as a function of fin

deflection angle for all three sets of data in the X, Y coordinates
explained in Figure 6. Information presented by Hayes in Reference 5
and data analyzed for this report strongly indicate that the shock
impingement location for the Langley and AEDC data coincides with
the indentation or trough in the pressure curve between the peak
and plateau pressure locations (illustrated in Figure 26). Thus,
the shock coordinates for the Langley and AEDC data were determined
on this basis. The Princeton shock locations were determined from
oblique shock theory but were verified with the pressure curves in
the manner explained above. The AEDC data conform to oblique shock
predictions as well (see Figure 22). Figure 29 shows the shock angle
as a function of fin deflection angle for various X/δ locations for
the Langley data. This plot demonstrates that the Langley shock
shape does not conform to oblique shock theory. (This is also illus-
trated in Figures 24 and 33). The reason for this difference in the
shock shape has not been determined. Figures 30 and 31 show the
location of disturbance onset (see Figure 2) for the Langley data
determined by two different methods. The AEDC and Princeton data
were not included because of the limited amount of data available.
Figure 30 shows the onset location determined by the intersection
point of the slope of the pressure curve in the undisturbed flow
region ($P/P_\infty = 1.0$) and the pressure curve between the onset and
separation regions. To determine how sensitive the onset location
is to change in pressure ratio, an arbitrary error of 10% was assumed
for the pressure ratio (i.e., $P/P_u = 1.1$). Figure 31 shows the onset

12

location determined by the intersection of the pressure curve with the $P/P_u = 1.1$ line. The onset location determined by the two methods were compared by plotting the Y/X value for the onset location determined by one method as a function of the Y/X location determined by the other method as shown in Figure 32. If the onset point determined by the two methods is the same, this plot will show a 1:1 relationship. From Figure 32 it can be seen that the data comparison does show a 1:1 ratio, indicating that either method is acceptable for determining the location of separation onset. Figure 33 shows the relative locations of the fin, shock, theoretical oblique shock, and disturbance onset for the Langley model for a fin deflection angle of 16 degrees.

b. Surface Effects Data

The effect of the interaction process on the surface pressures and heat transfer in the interaction region is shown in Figures 34 through 39. Figure 34 shows the normalized peak pressure and plateau pressure for all three groups of data as a function of nondimensional distance downstream from the fin leading edge (X/δ) for a fin deflection angle of 10 degrees. Figure 35 shows the normalized peak heating data for the same conditions. For comparison, this figure also shows the peak heating predicted by pressure interaction theory. It is obvious that pressure interaction theory does not adequately predict heating for a three-dimensional interaction. Figure 36 shows the normalized separation induced heating peak for

the Langley and AEDC data as a function of the shock strength parameter, $M_\infty \sin \Theta$. The Princeton data again were not included because the data instability precluded determining the location of the separation induced heating peak or its magnitude. Also shown is the curve fit of Nestler's data from Figure 19 of Reference 6. Figure 37 shows the same plot for the Langley data only. The difference between the two data plots is that the shock angle, Θ, is determined from oblique shock theory in Figure 36 and from the surface pressure data, as explained previously, in Figure 37. An error band of $\pm 10\%$ for the curve fit is also shown in both Figures 36 and 37. The figures show that the AEDC data are predicted very well by the curve fit but that the Langley data generally fall below the predicted values by more than 10%. It may be noted that Langley row 5 data differ markedly from the other data, particularly at the higher M_∞ $\sin \Theta$ values. An explanation of this behaviour has not been determined. Figure 38 shows the normalized heat transfer data on the flat plate at the shock impingement location for the Langley and AEDC data. As before, the Princeton data were not determinable because of its instability. Figure 39 shows the same plot for Langley data only. The difference between the two data plots is that in Figure 38 the shock location was determined from oblique theory, and in Figure 39, from pressure data. Figure 38 shows the surface heating under the shock to be constant up to a fin deflection angle of approximately 10 degrees and to then monotonically increase. This data trend was discussed by Neumann and Token in Reference 6 for data at Mach 3.7

14

and was explained as being due to incipient separation. The incipient separation angle for the Mach 3.7 data was approximately 6 degrees and was shown to correlate closely with Korkegi's simplified prediction. The data of Figure 38 was also compared to Korkegi's prediction (shown as the point where $M_\infty \alpha = 0.3$). Korkegi's method predicts incipient separation at approximately 6 degrees instead of the 10 degrees indicated by the data. Note, however, in Figure 39, that when the shock location is determined from the pressure data, the incipient separation angle is shown to decrease with normalized distance downstream from the leading edge, eventually approaching the angle predicted by Korkegi's method.

The parallel distribution of heating versus fin deflection for the increasing X/δ locations in Figure 39 rather than the fan-shaped distribution of Figure 38 may be due to the shock curvature evidenced when determining the shock location from the pressure data (see Figures 26 and 29). The shock curvature results in smaller y-values and correspondingly higher heating values. In addition, it can be seen from Figure 29 that shock curvature decreases with increasing fin deflection angle, approaching oblique shock values at fin deflection angles greater than 10 degrees. Thus, elevation of the heating values would tend to be greater at fin deflections less than 10 degrees thereby causing the curves to become parallel. It may be, therefore, that Korkegi's method is strictly applicable only for oblique shocks or far downstream for flows with shock curvature.

SECTION IV

CONCLUSIONS

The conclusion which can be drawn from the results of this investigation are as follows:

1. The distribution of normalized pressure and heat transfer data across the interaction region in a three-dimensional oblique shock/turbulent boundary layer interaction is independent of facility (i.e., Reynolds number) and model scale effects if the following conditions are met:

a. Mach number must be constant.

b. Pressure and heat transfer data must be normalized by the undisturbed flat plate values.

c. Pressure data must be compared at equal distances from the fin leading edge.

d. Heat transfer data must be compared at equivalent X/δ locations.

e. All data must be compared at comparable Y/X locations where Y and X have their origins at the fin leading edge (see Figure 1).

2. Additional data have been presented for the data base on the three-dimensional oblique shock/turbulent boundary layer interaction for use in helping to better understand the physics of the process.

16
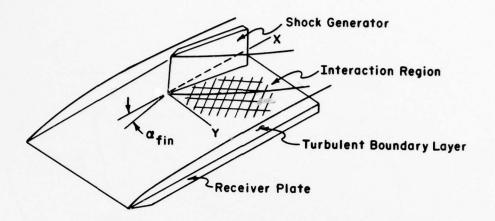
Figure 1.   General Interaction Region Type
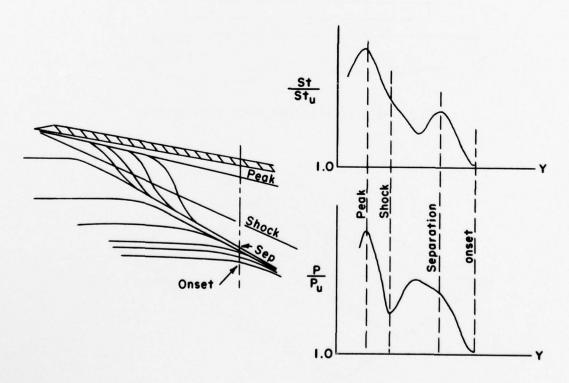
Figure 2.   Basic Interaction Characteristics
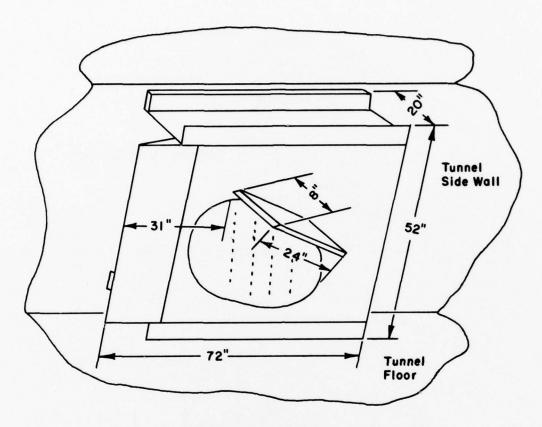
Figure 3.   NASA Langley UPWT Test Configuration
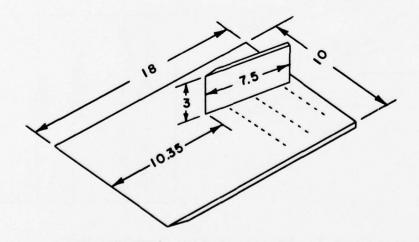
Figure 4.   AEDC Model Configuration
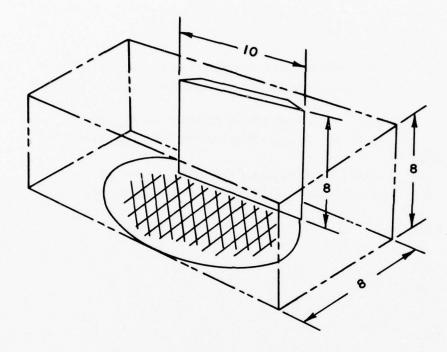
Figure 5.   Princeton Model Configuration
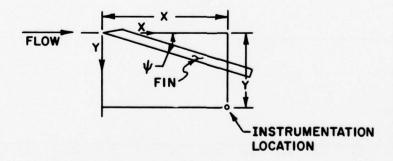
Figure 6.   Coordinate System for Data Comparison

19
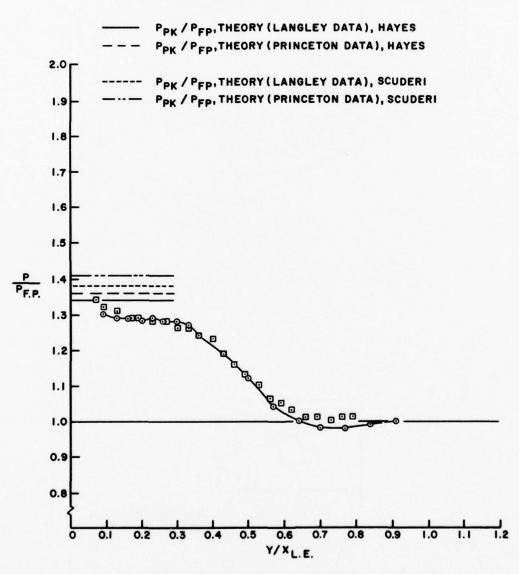
Figure 7. Comparison of Langley and Princeton Pressure Data for 4° Fin Deflection
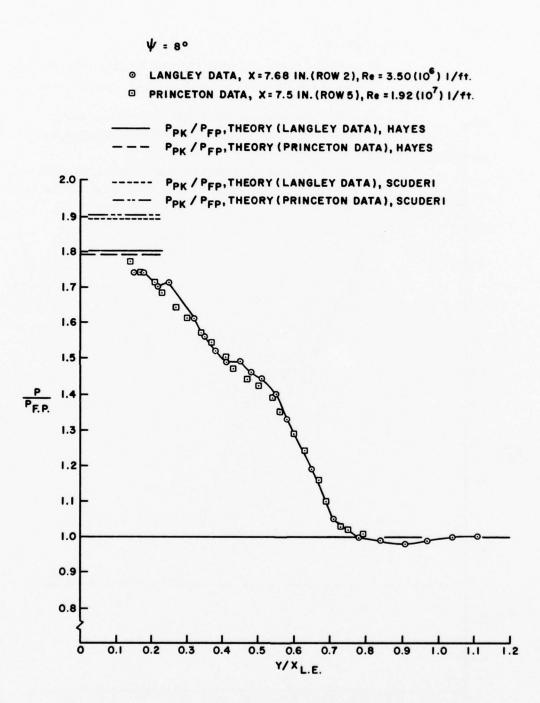
Figure 8.   Comparison of Langley and Princeton Pressure Data
for 8° Fin Deflection
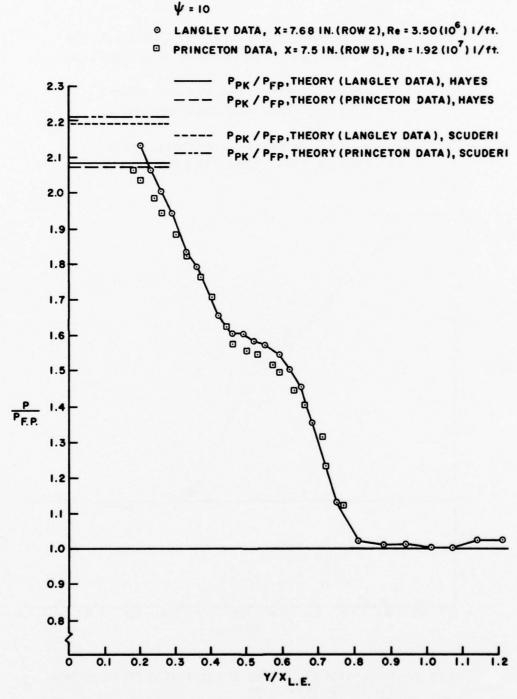
Figure 9. Comparison of Langley and Princeton Pressure Data
for 10° Fin Deflection
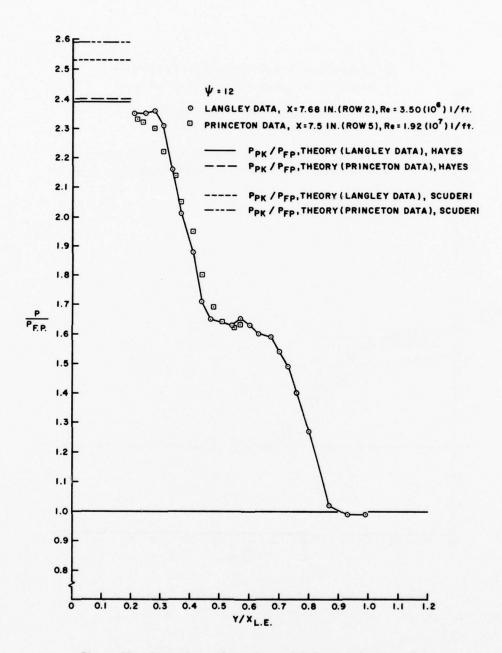
Figure 10.   Comparison of Langley and Princeton Pressure Data
for 12° Fin Deflection
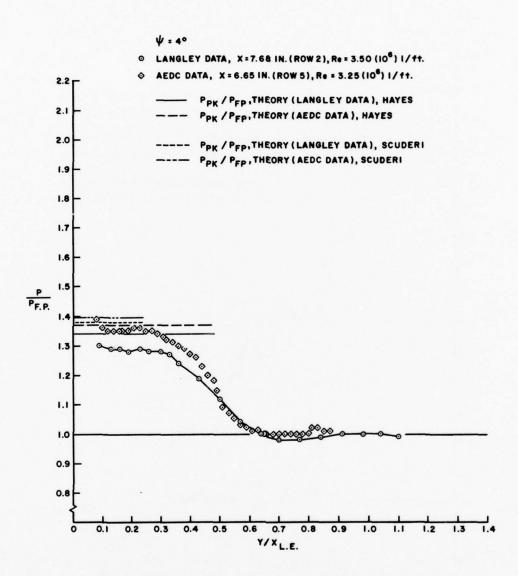
Figure 11. Comparison of Langley and AEDC Pressure Data
for 4° Fin Deflection
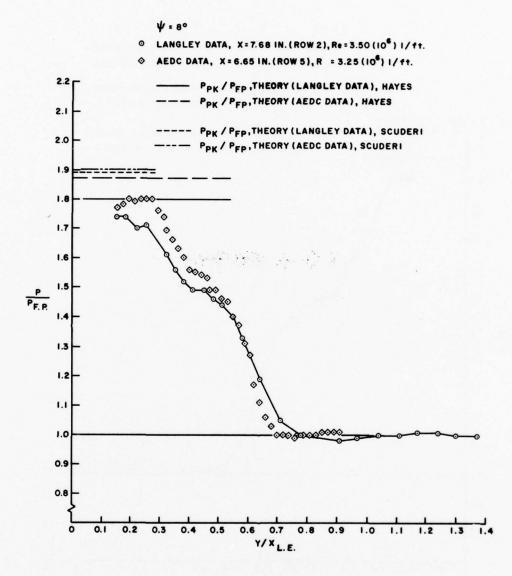
Figure 12. Comparison of Langley and AEDC Pressure Data
for 8° Fin Deflection

Figure 13. Comparison of Langley and AEDC Pressure Data
for 10° Fin Deflection
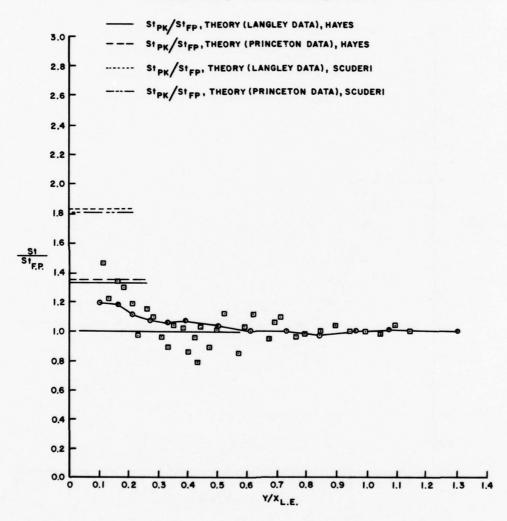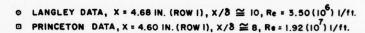
Figure 14.   Comparison of Langley and Princeton Heat Transfer Data
             for 4° Fin Deflection
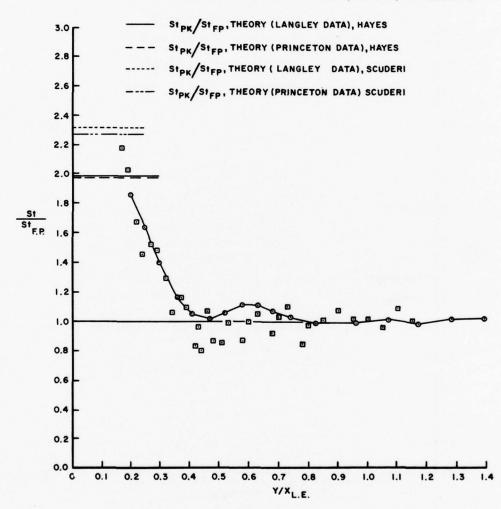
Figure 15. Comparison of Langley and Princeton Heat Transfer
Data for 8° Fin Deflection

Figure 16. Comparison of Langley and Princeton Heat Transfer Data for 10° Fin Deflection
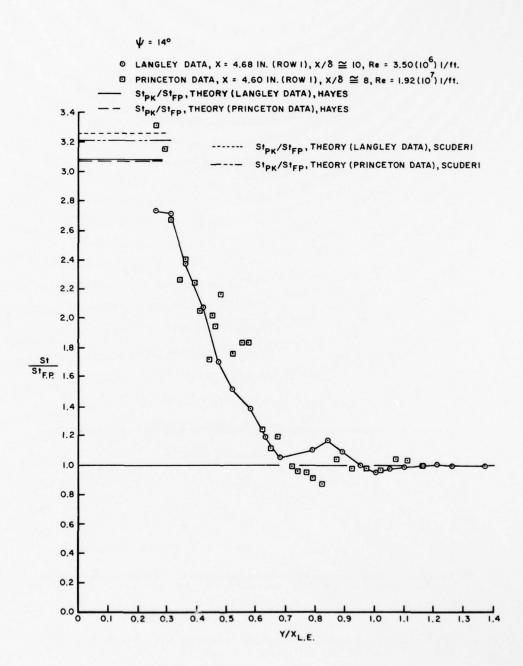
Figure 17. Comparison of Langley and Princeton Heat Transfer Data
for 14° Fin Deflection
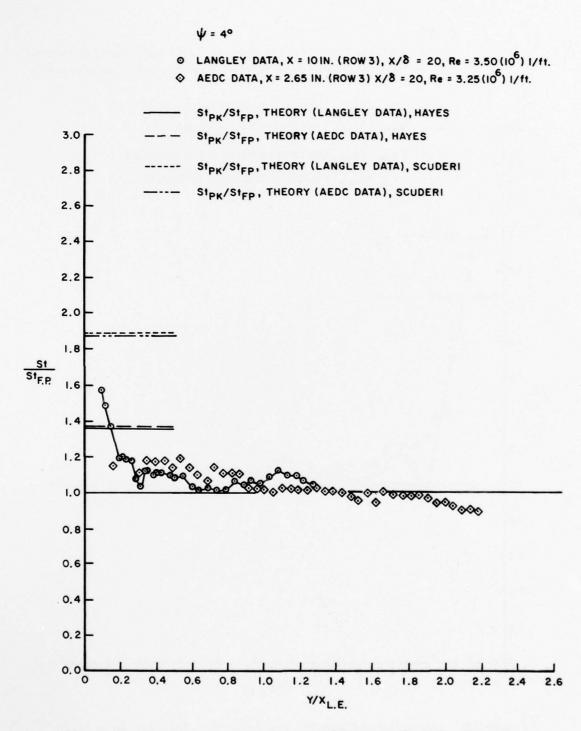
Figure 18. Comparison of Langley and AEDC Heat Transfer Data for
4° Fin Deflection
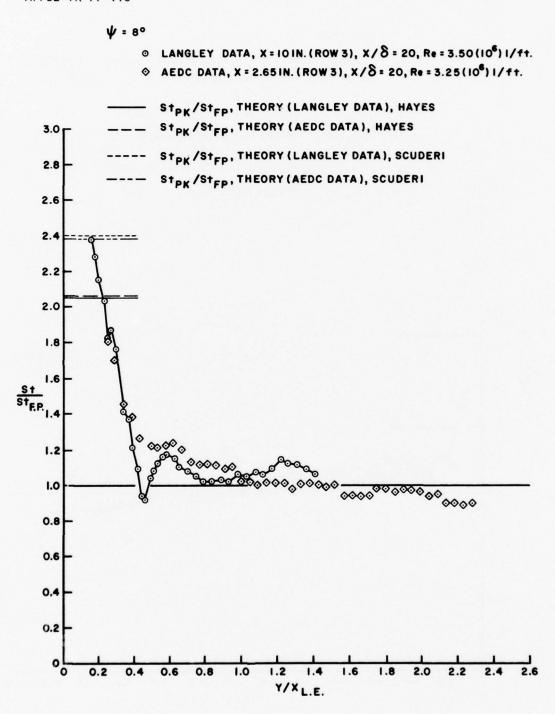
Figure 19. Comparison of Langley and AEDC Heat Transfer Data for 8°
Fin Deflection

$\psi = 10°$

⊙ LANGLEY DATA, X = 10 IN.(ROW 3), X/δ = 20, Re = 3.50 (10^6) 1/ft.

◇ AEDC DATA, X = 2.65 IN.(ROW 3), X/δ = 20, Re = 3.25 (10^6) 1/ft.

—— St_{PK}/St_{FP}, THEORY (LANGLEY DATA), HAYES

— — St_{PK}/St_{FP}, THEORY (AEDC DATA), HAYES

- - - - St_{PK}/St_{FP}, THEORY (LANGLEY DATA), SCUDERI

—·— St_{PK}/St_{FP}, THEORY (AEDC DATA), SCUDERI
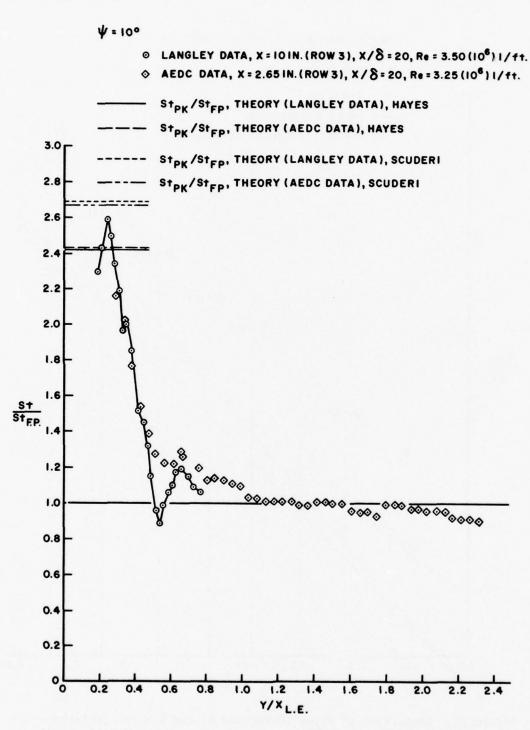
Figure 20. Comparison of Langley and AEDC Heat Transfer Data for 10° Fin Deflection
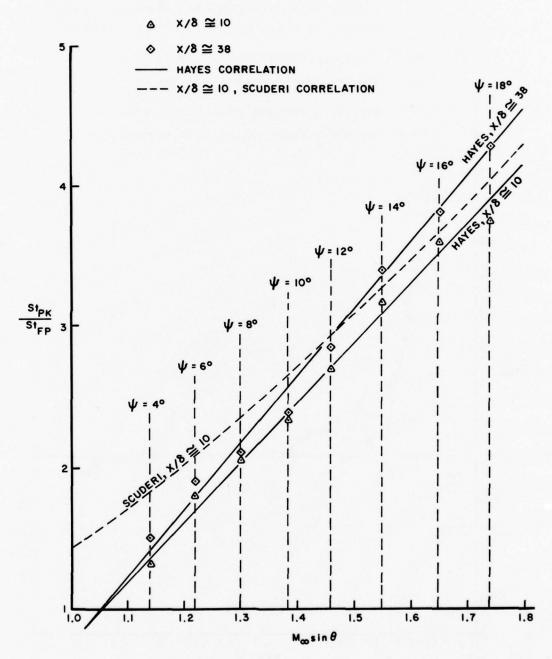
Figure 21. Comparison of Hayes (Reference 5) and Scuderi (Reference 10) Prediction Methods
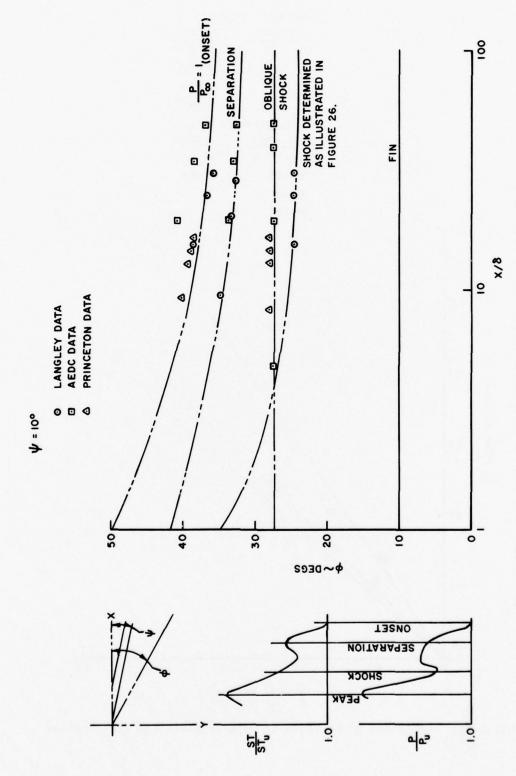
Figure 22. Geometric Characteristics of the Interaction Region
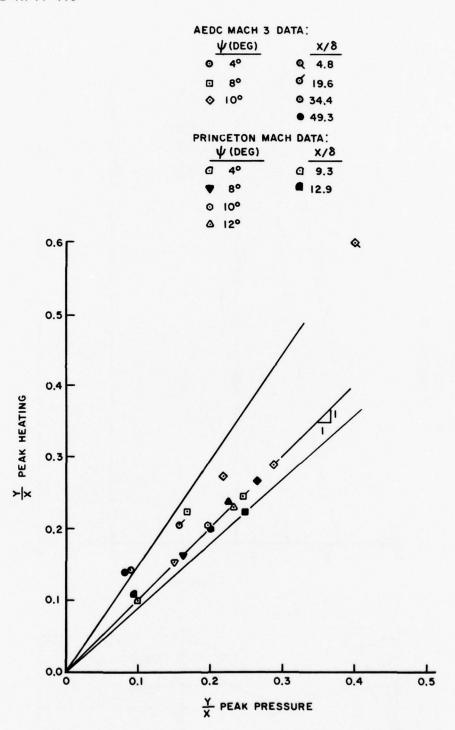
Figure 23.   Comparison of Location of Peak Pressure and Peak Heating
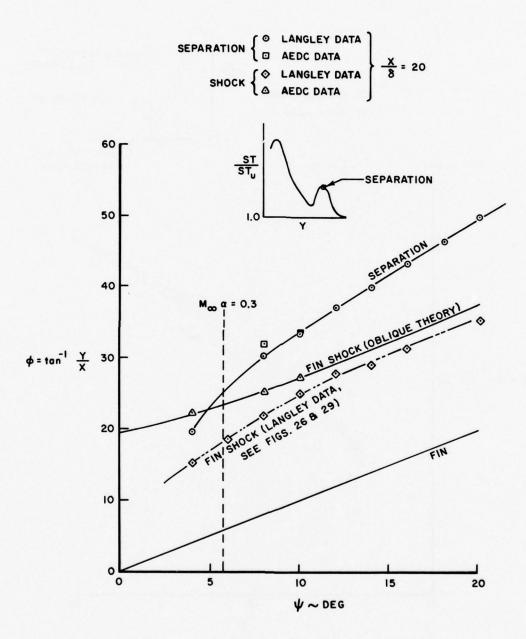
Figure 24. Angular Location of Separation as a Function of Fin Deflection Angle
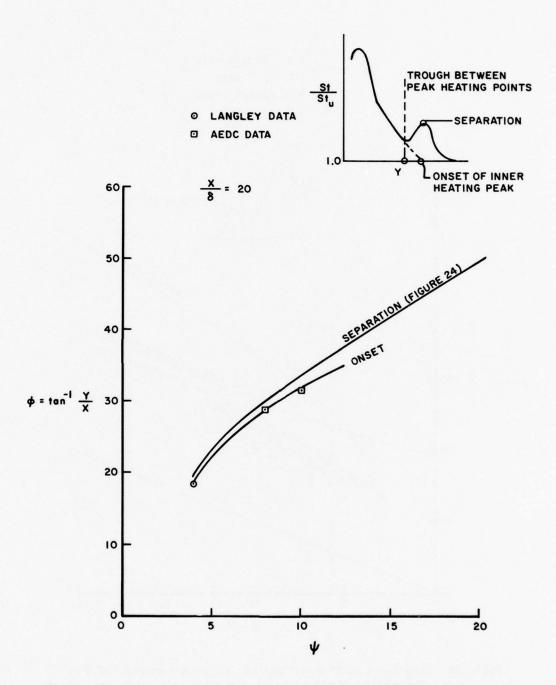
Figure 25. Comparison of Separation Location and Point of Onset of
Inner Heating Peak
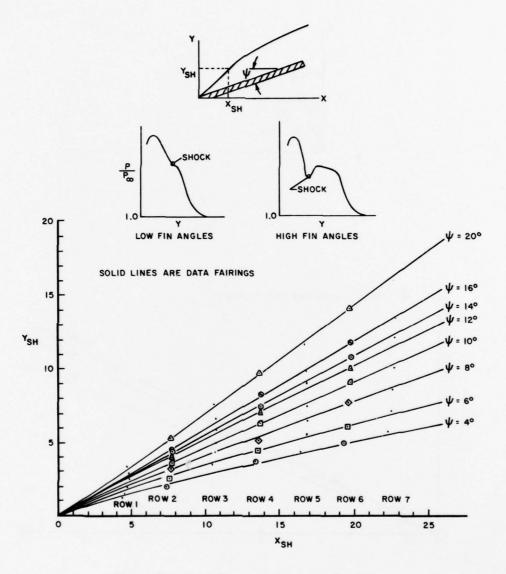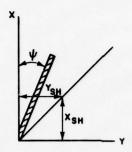
Figure 26.   Shock Wave Location - Langley Data
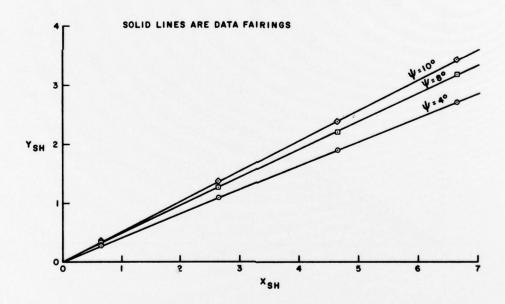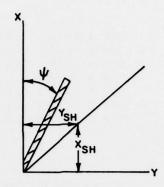
Figure 27. Shock Wave Location - AEDC Data

SOLID LINES ARE DATA FAIRINGS
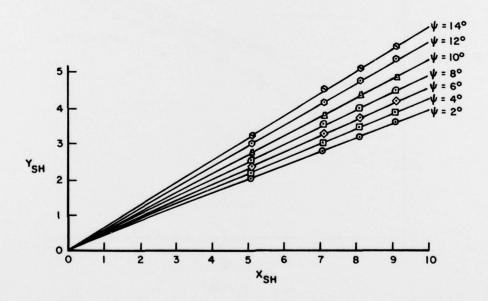
Figure 28.   Shock Wave Location - Princeton Data

41

ROW 1 (X/δ = 9.5)
▽ ROW 2 (X/δ = 15.6)
△ ROW 3 (X/δ = 20.4)
ROW 4 (X/δ = 25.0)
ROW 5 (X/δ = 28.6)
⊙ ROW 6 (X/δ = 32.2)
ROW 7 (X/δ = 34.9)
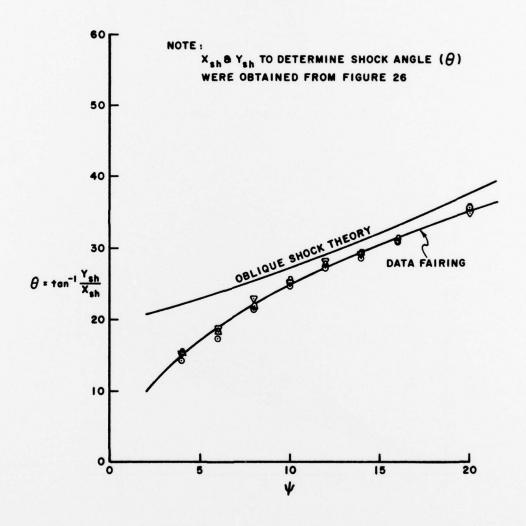
Figure 29. Shock Angle as Function of Fin Deflection Angle
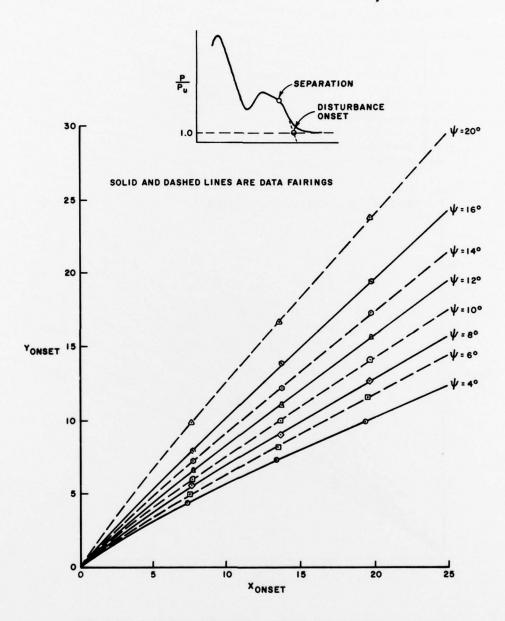
Figure 30.   Location of Disturbance Onset Based On Intersection
Point from Pressure Data
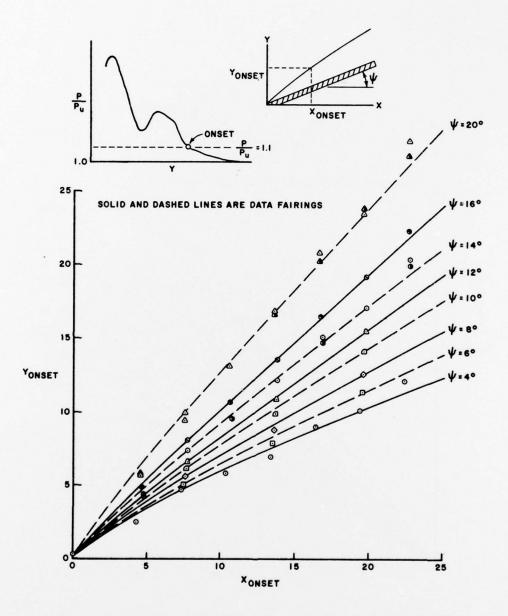
Figure 31. Location of Disturbance Onset Based on Location of Point Where $P/P_u = 1.1$
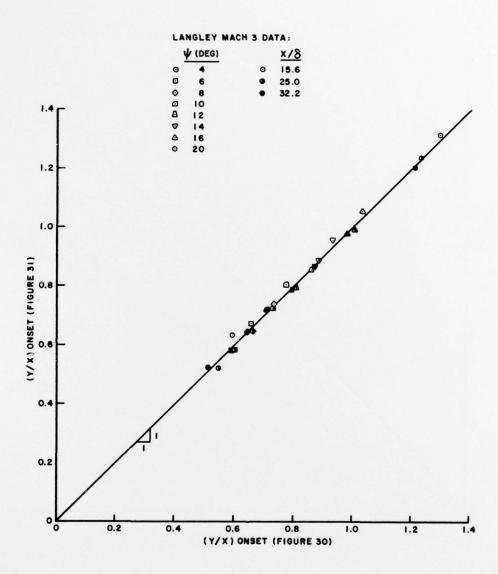
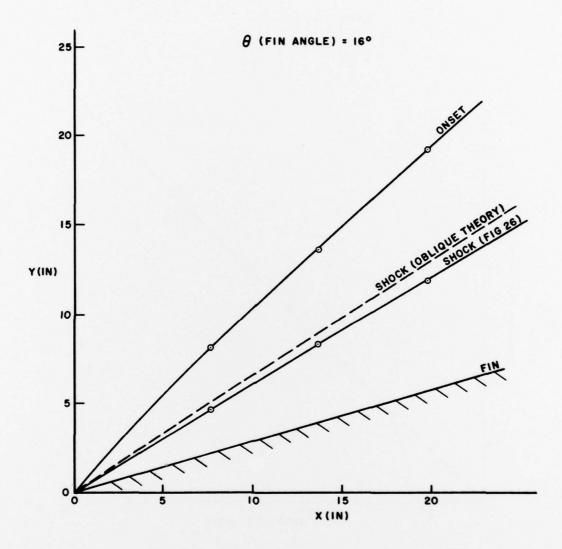Figure 32.   Comparison of Location of Disturbance Onset

Figure 33. Relative Location of Fin, Shock, Theoretical Oblique Shock, and Disturbance Onset for 16° Fin Deflection - Langley Data
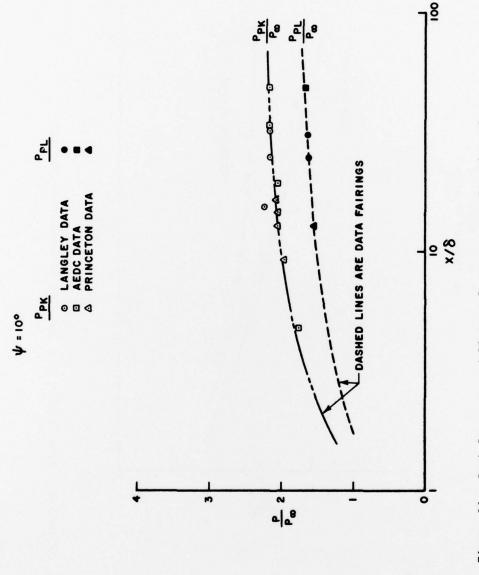
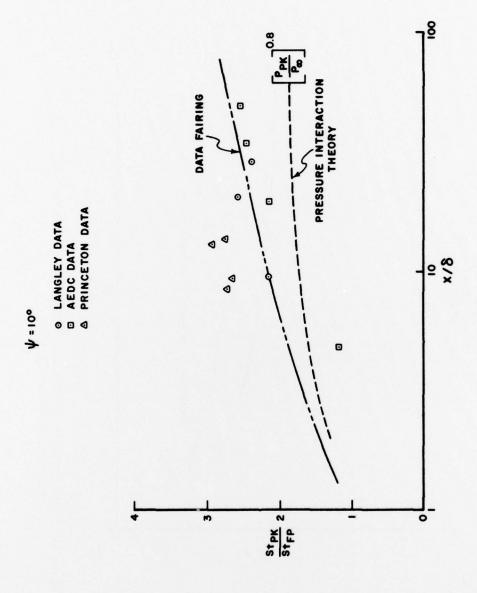Figure 34. Peak Pressure and Plateau Pressure as a Function of Downstream Distance

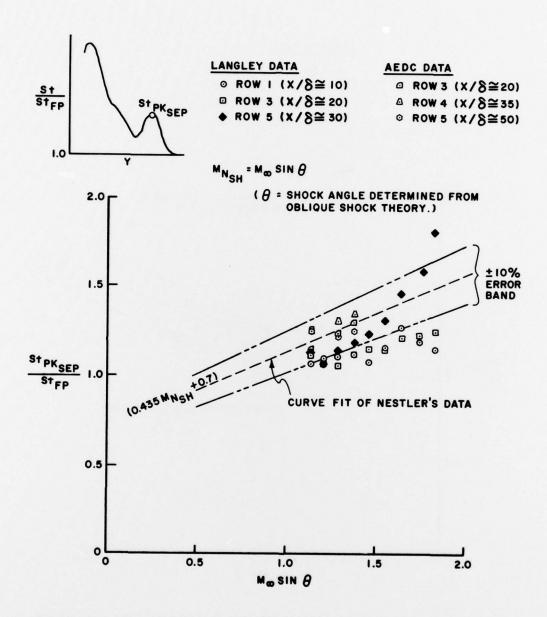Figure 35. Peak Heating as a Function of Downstream Distance

Figure 36. Magnitude of Separation Induced Heating Peak with Shock
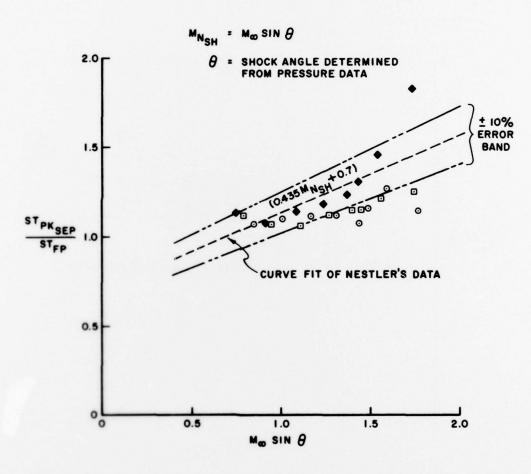Angle from Oblique Shock Theory

Figure 37. Magnitude of Separation Induced Heating Peak with Shock Angle from Pressure Data
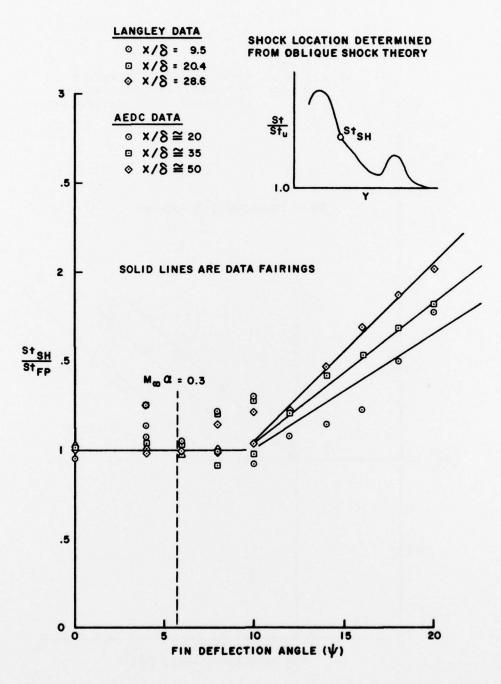
Figure 38. Magnitude of Heating at the Shock Impingement Location
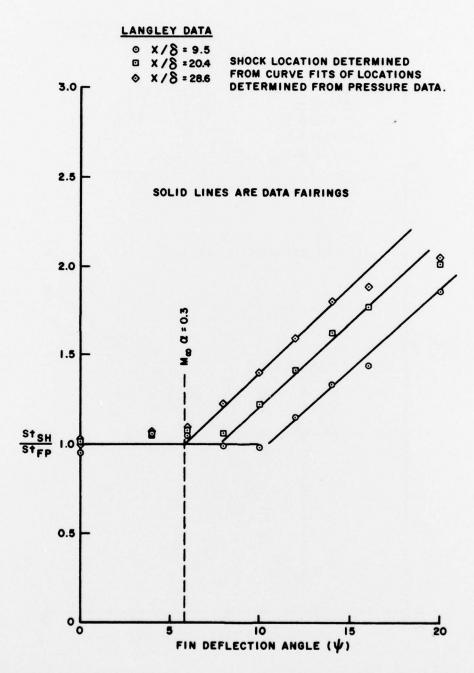with Shock Location from Oblique Shock Theory

Figure 39. Magnitude of Heating at the Shock Impingement Location with Shock Location from Pressure Data

REFERENCES

1. Stanbrook, A., "An Experimental Study of the Glancing Interaction Between a Shock Wave and a Turbulent Boundary Layer", Aeronautical Research Council C.P. No. 555, July 1960.

2. McCabe, A., "The Three-Dimensional Interaction of a Shock Wave with a Turbulent Boundary Layer", Aeronautical Quarterly, August 1966, pp. 231-252.

3. Lowrie, B. W., "Cross Flows Produced by the Interaction of a Swept Shock Wave with a Turbulent Boundary Layer", PhD Thesis, Univ. of Cambridge, December 1965.

4. Neumann, R. D., and Burke, G. L., "The Influence of Shock Wave-Boundary Layer Effects on the Design of Hypersonic Aircraft", AFFDL-TR-68-152, March 1969.

5. Hayes, J. R., "Prediction Techniques for the Characteristics of the Three-Dimensional Shock Wave Turbulent Boundary Layer Interaction", AFFDL-TR-77-10.

6. Neumann, R. D. and Token, K. H., "Prediction of Surface Phenomena Induced by Three-Dimensional Interactions on Planar Turbulent Boundary Layers", International Astronautical Federation XXVth Congress, Paper No. 77-46.

7. Korkegi, R. H., "On the Structure of Three-Dimensional Shock-Induced Separated Flow Regions", AIII Paper No. 76-165, January 1976.

8. Korkegi, R. H., "Simple Correlation for Incipient Turbulent Boundary Layer Separation Due to a Skewed Shock Wave", AIAA Journal, Vol. II, Nr. II, November 1973, pp. 1578-1579.

9. Holden, M. S., "Shock Wave-Turbulent Boundary Layer Interaction in Hypersonic Flow", A.R.L. 73-0137, October 1973.

10. Scuderi, L. F., "Procedures for Predicting Aerodynamic Heating and Surface Pressure Profiles Resulting from Three-Dimensional Shock Wave-Turbulent Boundary Layer Interactions", McDonnell Aircraft Co., Report Nr. MDC IR0015, December 1976.